# The transition from differentiation to growth during dermomyotome-derived myogenesis depends on temporally restricted hedgehog signaling

**Nitza Kahane[1], Vanessa Ribes[2,*], Anna Kicheva[2], James Briscoe[2] and Chaya Kalcheim[1,‡]**

## SUMMARY

The development of a functional tissue requires coordination of the amplification of progenitors and their differentiation into specific cell types. The molecular basis for this coordination during myotome ontogeny is not well understood. Dermomyotome progenitors that colonize the myotome first acquire myocyte identity and subsequently proliferate as Pax7-expressing progenitors before undergoing terminal differentiation. We show that the dynamics of sonic hedgehog (Shh) signaling is crucial for this transition in both avian and mouse embryos. Initially, Shh ligand emanating from notochord/floor plate reaches the dermomyotome, where it both maintains the proliferation of dermomyotome cells and promotes myogenic differentiation of progenitors that colonized the myotome. Interfering with Shh signaling at this stage produces small myotomes and accumulation of Pax7-expressing progenitors. An *in vivo* reporter of Shh activity combined with mouse genetics revealed the existence of both activator and repressor Shh activities operating on distinct subsets of cells during the epaxial myotomal maturation. In contrast to observations in mice, in avians Shh promotes the differentiation of both epaxial and hypaxial myotome domains. Subsequently, myogenic progenitors become refractory to Shh; this is likely to occur at the level of, or upstream of, smoothened signaling. The end of responsiveness to Shh coincides with, and is thus likely to enable, the transition into the growth phase of the myotome.

KEY WORDS: Avian embryo, Mouse, Gli, Myf5, Myotome, Somite

## INTRODUCTION

All body muscles derive from segmentally arranged somites (Christ and Scaal, 2008). These epithelial structures dissociate ventrally to form the sclerotome and medially to generate pioneer myocytes. By contrast, their epithelial aspect is preserved dorsally and constitutes the dermomyotome (DM) (Devoto et al., 2006; Kahane et al., 1998a; Scaal and Christ, 2004; Stellabotte and Devoto, 2007). The DM is a heterogeneous structure composed of both multipotent as well as fate-restricted progenitors giving rise to myocytes, smooth muscle, mitotic muscle progenitors, and also to dorsal dermis and endothelium of adjacent blood vessels (Ben-Yair and Kalcheim, 2008). Notably, segregation into these lineages occurs in a spatially and temporally regulated fashion (Nitzan and Kalcheim, 2013).

The DM is composed of a central sheet limited by four lips. Studies in avians showed that around embryonic day (E) 2.5 the lips generate myocytes (Cinnamon et al., 2006; Cinnamon et al., 1999; Gros et al., 2004; Huang and Christ, 2000; Kahane et al., 1998b; Kahane et al., 2002) that intercalate among a scaffold of earlier pioneer fibers and depend on integrity of this scaffold for proper patterning (Kahane et al., 1998a; Kahane et al., 2007). Similarly, progenitors delaminate from the central DM sheet and generate differentiated myocytes (Ben-Yair et al., 2011). Both pioneers as well as DM-derived myocytes express the myogenic regulatory factors *Myf5* and *MyoD* (also known as *Myod1*) (Buckingham,

2001). Subsequently, the central DM dissociates producing dermis and Pax3- and Pax7-positive myoblasts that remain mitotically active within the myotome and share a common lineage with dermal cells (Ben-Yair and Kalcheim, 2005; Buckingham and Montarras, 2008). Later, they develop into fibers or satellite cells, the adult muscle stem cells (Gros et al., 2005; Kassar-Duchossoy et al., 2005; Relaix et al., 2005). Hence, early muscle ontogeny is characterized by an initial patterning phase, during which the DM generates post-mitotic mononucleated fibers, followed by a growth phase, during which DM-derived cells retain a progenitor state. The transition between these two phases is temporally linked to DM dissociation (Ben-Yair and Kalcheim, 2005; Delfini et al., 2009) and depends on an LGN (the vertebrate homolog of partner of inscuteable; also known as Gpsm2)-mediated shift in mitotic orientation (Ben-Yair et al., 2011). However, the identity and mode of action of upstream factors that regulate this transition remain to be elucidated.

Sonic hedgehog (Shh) plays fundamental roles during early embryogenesis. Its signal is transduced via two transmembrane proteins, patched 1 (Ptc1; Ptch1) and smoothened (Smo), and culminates with the regulation of the activity of Gli transcription factors. These function either as transcriptional activators or repressors depending on the presence or absence of ligand, respectively (Ribes and Briscoe, 2009). During myogenesis, Shh was proposed to regulate precursor cell survival, proliferation and differentiation in a variety of vertebrates. In zebrafish, different levels and durations of Shh signaling specify distinct myotomal cell types (Feng et al., 2006; Hammond et al., 2007; Ingham and McMahon, 2001; Maurya et al., 2011; Wolff et al., 2003). In the chick, Shh was found to be necessary for epaxial but not limb muscle formation (Teillet et al., 1998), yet studies in mouse propose that it induces the myogenic program in the ventral limb (Anderson et al., 2012; Hu et al., 2012; Krüger et al., 2001). In addition, Shh has been shown to regulate *Myf5* expression in primary epaxial

[1]Department of Medical Neurobiology, IMRIC and ELSC, Hebrew University of Jerusalem-Hadassah Medical School, Jerusalem 91120, PO Box 12272, Israel.
[2]MRC-National Institute for Medical Research, Medical Research Council, London, NW7 1AA, UK.

*Present address: UPMC Paris 06, UMR-S 787, F-75013, Paris, France
‡Author for correspondence (kalcheim@cc.huji.ac.il)

myoblasts (Borycki et al., 1999; Chiang et al., 1996; Gustafsson et al., 2002), although other studies do not support this finding (Teboul et al., 2003). Notably, in $Shh^{-/-}$ embryos $Myf5$ expression is induced, but not maintained, and epaxial muscles are not formed (Borycki et al., 1999). Furthermore, Gli2 and Gli3, essential effectors of Shh signaling in somites (Ingham and McMahon, 2001; Sasaki et al., 1997), influence the dynamics of $Myf5$ expression (Buttitta et al., 2003; McDermott et al., 2005). Finally, ectopic application of Shh causes premature myoblast differentiation at the expense of $Pax3$ expression (Amthor et al., 1999; Blagden and Hughes, 1999; Borycki et al., 1999; Du et al., 1997; Kahane et al., 2001).

In this study, we used mouse genetics and spatiotemporal manipulations of gene expression in avians to investigate mechanisms of myoblast differentiation and transition into the growth phase. Using chick embryos, we provide evidence that Shh spreads from midline structures through the sclerotome to reach the DM/myotome. There it promotes terminal myogenic differentiation of both epaxial and hypaxial DM-derived progenitors and maintains proliferation of DM cells. Strikingly, the ability of Shh ligand to promote differentiation is time limited such that when the myotome enters its growth phase progenitors become unresponsive to Shh ligand, an event occurring at the level of, or upstream of, signal reception. Consistent with this, analysis of an *in vivo* reporter for Shh/Gli signaling in mice revealed that Gli activity is only transiently upregulated in the epaxial myotome. Analysis of several mouse mutants shows that the spatial and temporal dynamics of reporter activity are shaped by both activator and repressor functions of Gli proteins. Altogether our data support a model in which the loss of responsiveness of the DM-derived muscle progenitors to Shh is a key mechanism by which the myotome transits from differentiation into expansion.

## MATERIALS AND METHODS
### Avian embryos and mouse lines
Fertile chick (*Gallus gallus*) and quail (*Coturnix coturnix Japonica*) eggs were from commercial sources. The *Tg(GBS-GFP)* mouse line was generated as described (Balaskas et al., 2012). Mice containing mutant alleles for *Shh* null and *Gli3* ($Xt^J$ allele) were described previously (Hui and Joyner, 1993; Lewis et al., 2001). Genotyping was carried out as reported (Büscher et al., 1998; Lewis et al., 2001). Embryonic day (E) 0.5 was the day vaginal plugs were found. All procedures were carried out with the approval of the Institute Ethical and Biological Services Animal Research Committees under Home Office Project License (PPL 80/2091).

### Expression vectors and electroporation
The following expression vectors were employed: pCAGGS-AFP (Momose et al., 1999), PTC$^{\Delta loop2}$ (Briscoe et al., 2001), MyoD (Delfini and Duprez, 2004), Gli3A Medium (Stamataki et al., 2005), SmoM2 (Hynes et al., 2000), Rat Shh (from A. Klar, The Hebrew University of Jerusalem), and Hhip (Chuang and McMahon, 1999); to achieve conditional expression, the latter was subcloned into pBI (pTRE) and co-electroporated along with pCAGGS-rtTA2s-M2 (Watanabe et al., 2007).

For electroporations, DNA (1-4 µg/µl) was microinjected into the center of flank-level epithelial somites. Electroporations were performed to the ectoderm, and to the medial, lateral, dorsal and ventral parts of the epithelial somites [prospective pioneers, ventrolateral lip (VLL), DM and sclerotome, respectively]. Medial and lateral electroporations were performed by inserting sharpened tungsten electrodes into the coelomic cavities on both sides of the embryo. For ventral-to-dorsal transfections, the negative electrode was inserted under the endoderm and the positive dorsal to the ectoderm (Ben-Yair et al., 2011; Halperin-Barlev and Kalcheim, 2011; Kahane et al., 2007). For ectoderm transfections, DNA was injected between the embryo and extra-embryonic membranes and electric current applied in a dorsoventral direction. A four parameter PulseAgile square wave

electroporator (PA-4000, Cyto Pulse Sciences) was used. One pulse of 12V was applied for 10 mseconds. Some electroporated embryos received a pulse of bromodeoxyuridine (BrdU; 10 mM) for 1 hour prior to fixation.

### Grafting of pluronic gel
Pluronic F-127 gel was prepared as described (Groysman et al., 2008) and mixed with 400 µM cyclopamine (from a 20 mM stock in DMSO) or with DMSO alone. Gel drops were placed dorsal to the embryo at the level of epithelial somites, and replaced every 4-5 hours, for a total incubation period of 14-16 hours.

### Notochord grafts
Notochord (No) fragments were excised from E2 quail embryos (Charrier et al., 2001). A slit was made through the flank-level ectoderm of E2 or E3 embryos dorsal to the somite or DM, respectively, followed by tissue grafting.

### Tissue processing, immunohistochemistry and *in situ* hybridization
Mouse embryos were fixed in 4% formaldehyde for 45 minutes to 2 hours at 4°C. Fixed embryos were cryoprotected by equilibration in 15% sucrose, cryosectioned (14 µm), and processed for immunostaining with antibodies to GFP (Biogenesis), Arx (from J. Chelly, Institut Cochin, INSERM and CNRS, Paris) and Pax7 [Developmental Studies Hybridoma Bank (DSHB)].

Avian embryos were fixed with 4% formaldehyde, and either embedded in paraffin wax and sectioned at 8 µm, or observed as whole-mount preparations. Immunostaining for GFP and desmin (Molecular Probes), Pax7 and myosin (MF20, DSHB), and BrdU was as described (Kahane et al., 2001). Nuclei were visualized with Hoechst or DAPI.

For *in situ* hybridization (ISH), a chicken *Gas1* probe was generated by PCR using the following primers: ACATCTAGAGCCGTGTGTCT-GTAGAGATTTGAC (5′) and ACAGTCGACTCAGCACCCTGATA-CGACAAGAGG (3′). Additional probes were: *MyoD*, *Myf5* (Pownall and Emerson, 1992), *Gli1*, *Gli2*, *Gli3*, *Ptc1* (Borycki et al., 1998), *Cdo*, *Boc* (from the BBSRC ChickEST Database) (Boardman et al., 2002), *Hhip* (Chuang and McMahon, 1999) and *Sulf1* (Danesin et al., 2006). ISH was performed as described (Cinnamon et al., 2001).

Whole-mounts and sections were photographed using a DP70 (Olympus) cooled CCD digital camera mounted on a BX51 microscope (Olympus). Confocal scanning was carried out using an Olympus Fluoview FV1000, software version 1.7c. For figure preparation, images were exported into Photoshop CS2 (Adobe). If necessary, the brightness and contrast were adjusted to the entire image. In all transverse sections presented, lateral is to the left and dorsal is top.

### Data analysis and statistics
The number of myotomal cells co-expressing Pax7 and GFP was counted in every second section of entire segments. Myotomes were defined by desmin staining, and cells identified by the presence of Hoechst$^+$ or DAPI$^+$ nuclei. Results are expressed as percentage of total GFP$^+$ transfected cells. The area occupied by desmin$^+$ myotomes was measured using ImageJ software. Significance of results was determined using the non-parametric Mann–Whitney test. All tests applied were two-tailed, and a *P*-value of 0.05 or less was considered statistically significant.

## RESULTS
### Dynamics of Shh signaling during DM-derived trunk myogenesis in chick and mouse
#### Expression of Shh pathway components and interactors in the chick DM and/or myotome
*In situ* hybridization (ISH) for several Shh pathway components was performed on E2.5 chick embryos at the thoracic level. At this stage, the myotome contained only post-mitotic myocytes and the DM was epithelial. *Gli1*, *Gli2* and *Gli3* were transcribed throughout the DM, whereas *Gli1* and *Gli2*, but not *Gli3*, were also in the myotome (Fig. 1A-C). Both *Ptc1* and *Hhip*, two transcriptional
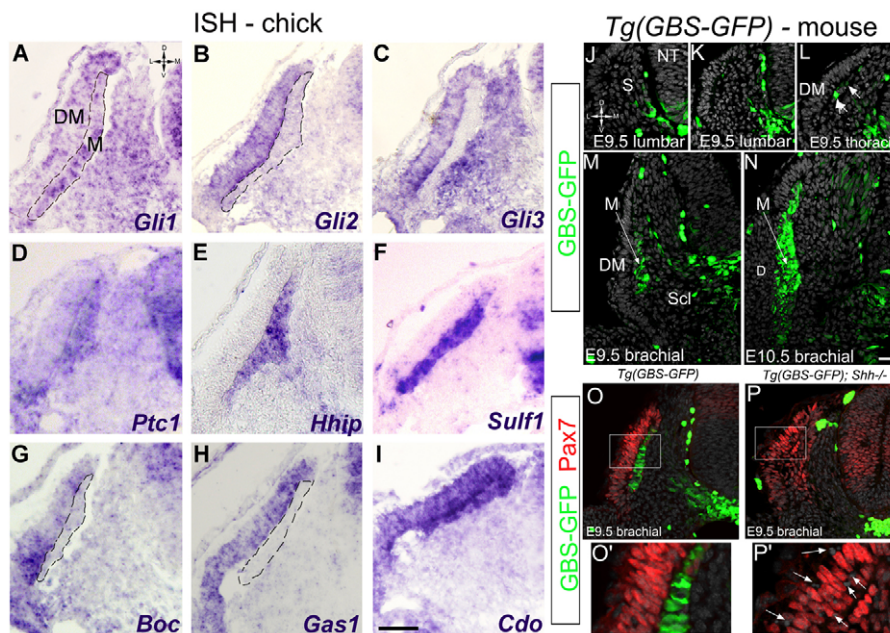
**Fig. 1. Shh and Gli activity in the DM and myotome of chick and mouse embryos.** (**A-I**) ISH on the flank of E2.5 chick embryos. *Gli1-3*, *Boc*, *Gas1* and *Cdo* are expressed in DM; *Ptc1*, *Hhip*, *Sulf1* and *Cdo* and low levels of *Gli1* and *Gli2* are in myotome. Dashed lines mark the myotome. (**J-P′**) GFP, Pax7 and DAPI (gray) staining on *Tg(GBS-GFP)* control or *Shh⁻/⁻* mouse embryos at the indicated stages and axial levels. O′ and P′ are higher magnifications of boxes in O and P, respectively. Arrows in L-N point at myotomal cells, those in P′ to pyknotic nuclei. All pictures are transverse sections. D, dermis; DM, dermomyotome; M, myotome; NT, neural tube; S, somite; Scl, sclerotome. Scale bars: 50 μm.

targets of Shh signaling (Chuang and McMahon, 1999; Ingham and McMahon, 2001) were transcribed in the myotome (Fig. 1D,E). Furthermore, *Gli1*, *Gli3*, *Ptc1* and *Hhip* were also weakly transcribed in sclerotome. Sulfatase 1 (*Sulf1*), a known Shh target in myogenic progenitors (Dhoot et al., 2001), was also transcribed in the myotome (Fig. 1F). Finally, the Shh-interacting co-receptors *Boc*, *Gas* and *Cdo* (Allen et al., 2011; Izzi et al., 2011) were expressed in DM and *Cdo* was also expressed in the myotome (Fig. 1G-I). Notably, upon DM dissociation and transition into the growth phase (E3.5 onwards), expression of all markers was reduced (data not shown). Thus, key components of Shh signaling are transcribed transiently in the DM and/or myotome raising the possibility that Shh signaling operates on these primordia. Furthermore, the high expression levels of the direct Shh targets *Hhip*, *Ptch1*, *Gli1* and *Sulf1* in the myotome testify that Shh signaling is particularly active within this tissue.

### The spatiotemporal sequence of myotome maturation and Shh/Gli activity in mouse embryos

To characterize the dynamics of Shh signaling further and to correlate this with the differentiation program, we used a mouse reporter line, *Tg(GBS-GFP)*, in which GFP expression is induced by the binding of Gli proteins to a concatamer of Gli-binding sites (Balaskas et al., 2012). Consistent with expression of the direct Shh target genes *Ptc1* and *Gli1* in chick and mouse myotomes (Fig. 1; supplementary material Fig. S1), the GFP signal was detected in myotomal cells at the thoracic level from E9.5 onwards (Fig. 1J-L, arrows) (supplementary material Fig. S1). In addition, a medial-to-lateral gradient of decreasing *Tg(GBS-GFP)* activity was clearly apparent in the sclerotome at E9.5 (Fig. 1J-O), resembling that of *Gli1* and *Ptc1* transcripts (supplementary material Fig. S1). Moreover, GBS-GFP signal was completely absent in both myotome and sclerotome of *Shh⁻/⁻* embryos, further demonstrating that this reporter reflects Shh activity (Fig. 1O-P′). Together, these data provide evidence of graded Shh signaling in the sclerotome and of dynamic activity in the myotome. Moreover, in spite of weak or no sclerotomal GFP signal next to the myotome, *Tg(GBS-GFP)* activity in muscle primordia was surprisingly high (Fig. 1M,N).

This suggests that Shh, which is expressed within the notochord and floor plate, spreads through the sclerotome to reach the DM/myotome.

We next compared the activity of the *Tg(GBS-GFP)* reporter with the expression patterns of myotomal genes. In mouse, Pax7⁺ progenitors are apparent in the myotome at E9.5 when the overlying DM is still epithelial (Fig. 2A). This differs from avians, in which the early myotome is devoid of Pax7⁺ cells (Kahane et al., 2001). By E10.5, most Pax7⁺ progenitors were localized in the medial myotome, abutting the sclerotome, whereas the lateral myotome, adjacent to the dermis, contained differentiated myocytes expressing the transcription factor Arx (Biressi et al., 2008) and/or myosin (Fig. 2B,B″,C). Likewise, a GFP-encoding plasmid focally electroporated into the medial epithelial somite of E2 quail embryos to mark pioneer myoblasts (Kahane et al., 1998a; Kahane et al., 1998b; Kahane et al., 2002) was expressed 2 days later in the lateral portion of the desmin⁺ myotome. By contrast, younger GFP⁻/desmin⁺ myoblasts were localized more medially abutting the sclerotome (*n*=15 with 50-60 transfected fibers/segment; Fig. 2F). Hence, both mouse and avian myotomes mature in a lateral-to-medial direction.

Strikingly, *Tg(GBS-GFP)* activity was enriched in the medial region of the myotome where most Pax7⁺ progenitors were located. Conversely, it was largely absent from the lateral myotome, which contained differentiated myocytes expressing Arx and/or myosin (Fig. 2B,C), although a few cells co-expressing Arx and GBS-GFP protein could be detected (Fig. 2D‴). This suggests that once they have differentiated, myocytes do not require Shh signaling. In addition, we noticed that in the *Tg(GBS-GFP)*-positive myotomal region some Pax7⁺ cells were negative for both the reporter activity (Fig. 2B-B″,D-D″) and Arx (Fig. 2). This indicates that although some progenitors differentiate, others remain in a Pax7⁺ state up to at least E12.5 (Fig. 2G).

Finally, from this stage onwards, the levels of GBS-GFP protein were substantially downregulated (Fig. 2E). Analysis of the distribution of *GFP* transcripts, which have a shorter half-life than that of the protein (Balaskas et al., 2012), demonstrated that the downregulation of Shh signaling is likely to occur with the rostral
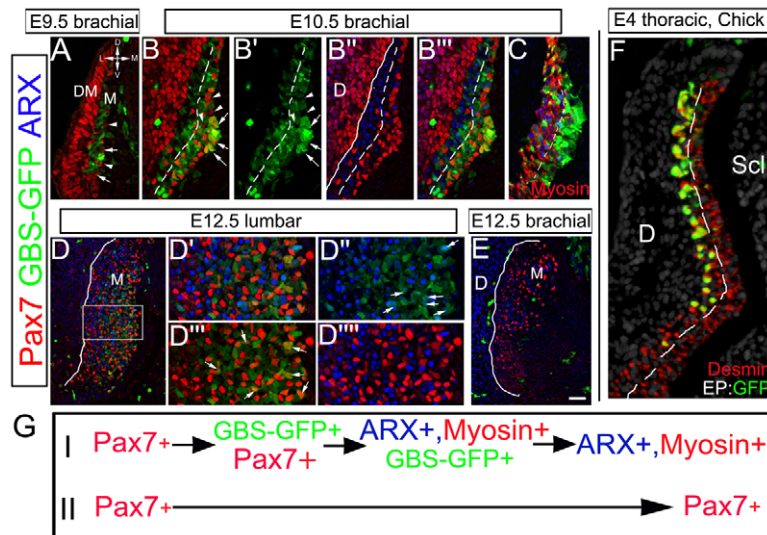
**Fig. 2. The dynamics of Gli activity defines the sequential development of the mouse myotome.** (**A-E**) Immunostaining for Pax7, Arx, GFP or myosin on *Tg(GBS-GFP)* mouse embryos at the indicated stages and axial levels. B-B‴ are the same image with different marker combinations. Arrows point at Pax7^{+}/GFP[+] or ARX[+]/GFP^{+} cells, arrowheads Pax7^{+}/GFP^{−} cells. Dashed lines separate the differentiating, Gli-responsive medial part of the myotome from its more differentiated Arx[+] lateral part. D-D‴ are higher magnifications of D showing that Arx and Pax7 are mutually exclusive (D‴) and that subsets of Arx[+] and Pax7^{+} populations express low levels of GFP (D′-D‴). By E12.5, GBS-GFP signal is downregulated at brachial levels (E). Unbroken lines in B″, D and E mark the border between myotome and dermis. (**F**) Immunostaining for GFP and desmin on E4 chick embryo, in which the medial part of a somite has been electroporated with GFP-DNA at E2. GFP[+]/Desmin[+] pioneer fibers occupy the lateral part of the myotome; younger desmin[+]/GFP[−] myocytes its medial domain. (**G**) Progression of molecular identities during maturation of two distinct myoblast populations. D, dermis, DM, dermomyotome, M, myotome, Scl, sclerotome. Scale bars: in A-C, 100 µm; in D,E, 200 µm; in F, 50 µm.

regions of the E11.5 embryos (supplementary material Fig. S1). Consistent with this, the levels of *Gli1* and *Ptc1* mRNA in the mouse myotome were downregulated (supplementary material Fig. S1). Altogether, these data confirm that Shh/Gli activity is switched off from E11.5 within the myotome.

The preceding data suggest a sequence of cell maturation in the myotome that correlates with changes in Shh signaling. A subset of Pax7^{+} progenitors displays transient high levels of Shh signaling and generates differentiated myocytes. During their differentiation, these cells downregulate Pax7, upregulate Arx and myosin, and turn down Shh signaling. A second subset of myotomal progenitors that express Pax7 but are negative for Gli activity and myogenic differentiation markers is likely to represent enduring precursors that will also generate satellite cells (Fig. 2G). This might indicate that in the mouse, both differentiating and non-differentiating myoblasts co-exist in the myotome during the differentiation phase. Because at every stage we detected progenitors that expressed only Pax7, the possibility exists that this cell population is established in the myotome early and is refractory to Shh throughout development.

## A role of Shh signaling in regulating DM-derived trunk myogenesis
### Shh cell-autonomously promotes myogenic differentiation of the epaxial and hypaxial domains of the avian myotome
Although a direct myogenic effect of Shh signaling on the zebrafish DM to produce a subset of fast fibers has been shown (Feng et al., 2006; Hammond et al., 2007), roles for Shh signaling within the DM and/or during DM-dependent myogenesis remain largely unexplored in amniotes. To address this issue, we first inhibited Shh signaling using cyclopamine, a small molecule antagonist of Smo (Incardona et al., 1998) from E2.5 when the pioneer myotome is already formed

and the DM begins contributing to the myocyte pool. Sixteen hours later, a marked reduction of myotomal size was apparent in cyclopamine-treated embryos (*n*=8) compared with controls (*n*=9; Fig. 3A-H) with fewer fibers expressing desmin (Fig. 3A,B) and fewer cells transcribing *Myf5* and *MyoD* (*n*=4, for each treatment; Fig. 3E-H). Instead, many myotomal cells remained Pax7^{+} (*n*=6; Fig. 3D,D′), whereas in controls the proportion of these progenitors was much smaller (*n*=7; Fig. 3C,C′). In addition, cyclopamine treatment led to premature dissociation of the central DM (Fig. 3C,D).

To examine whether Shh acts on the DM directly or indirectly, Shh signaling was abrogated by electroporating DM cells with a dominant-active version of *Ptc1* (PTC$^{\Delta loop2}$) (Briscoe et al., 2001). Electroporations were performed at E2 and the fate of transfected cells was analyzed either after 24 hours (Fig. 3I-N) or 44 hours (Fig. 3O-T); the later stage allowed us to assess formation of the lateral myotome, which appears later than the medial myotome (Cinnamon et al., 1999). After 24 hours, DM progenitors electroporated with control GFP remained mostly within the epithelium and some were extruded into the myotome where they lost Pax7 expression and generated fibers (Ben-Yair et al., 2011) (Fig. 3I-K,U; *n*=5). By contrast, overexpression of PTC$^{\Delta loop2}$ into the medial DM significantly increased the proportion of Pax7^{+} cells in the myotome (*n*=7; *P*<0.003; Fig. 3L-N,U). Moreover, overexpression of *PTC*$^{\Delta loop2}$ in the lateral DM had similar effects (*n*=5; *P*<0.003; Fig. 3O-T,U).

To determine whether inhibition of Shh signaling affects the mitotic activity of muscle progenitors, we monitored BrdU incorporation in control and PTC$^{\Delta loop2}$-treated embryos. In control GFP-electroporated myotome cells, 17.8±1% of nuclei incorporated BrdU whereas this percentage increased to 25±2.7% upon ectopic expression of PTC$^{\Delta loop2}$ (*P*<0.016; *n*=4 and 5, respectively). This suggests that the lack of Shh activity maintains myotomal
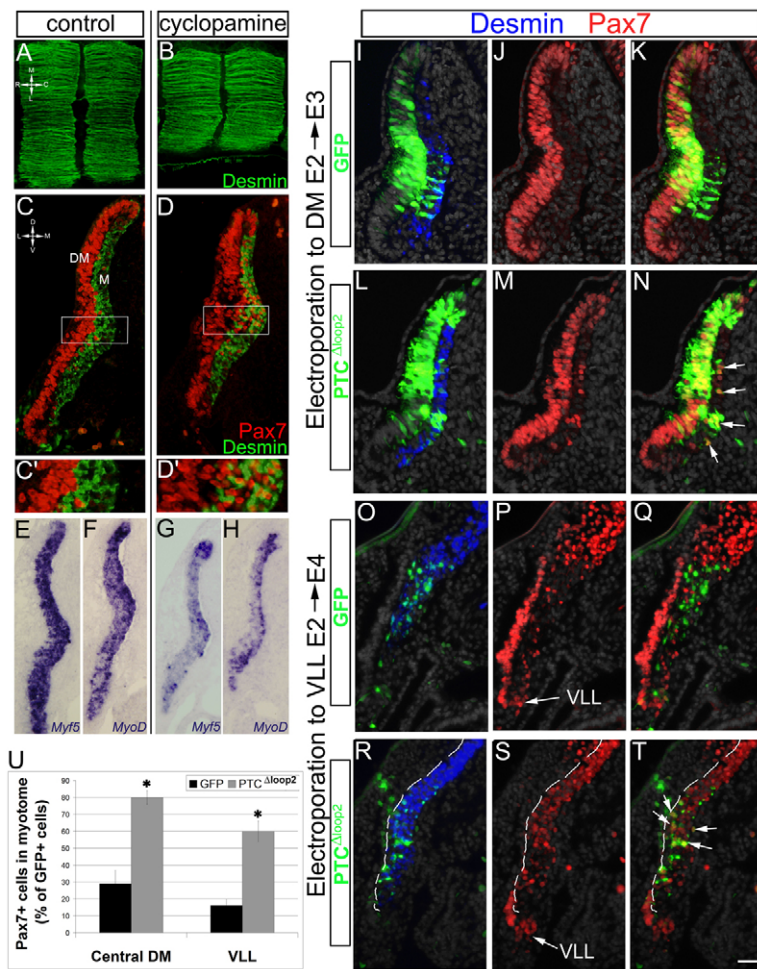
**Fig. 3. Shh is necessary to trigger the differentiation of Pax7+ DM-derived progenitors.** (**A-H**) E2.5 embryos subjected for 16 hours to pluronic gel alone (control) or cyclopamine in pluronic gel. Desmin+ myotomes were smaller in the presence of cyclopamine (dorsal views in A,B), contained more Pax7+ progenitors (C,D and higher magnifications in C′,D′), and exhibited reduced expression of *Myf5* and *MyoD* mRNAs (E-H). (**I-T**) Expression of PTC$^{\Delta loop2}$ cell-autonomously represses myogenic differentiation in both the medial (I-N) and lateral (O-T) myotome. (**U**) Quantification of the percentage of Pax7+ cells in myotome out of total GFP+ cells. *$P<0.003$. Error bars represent s.e.m. Dashed line in R-T represents the lateral limit of the desmin+ myotome. DM, dermomyotome; M, myotome; VLL, ventrolateral lip. Scale bar: in C,D,O-T, 50 μm; in E-H, 60 μm; in I-N, 40 μm.

progenitors in a mitotically active Pax7+ state. Conversely, the proportion of GFP+/BrdU+ nuclei in the DM dropped from 52±1.2% to 39±2.5% upon PTC$^{\Delta loop2}$-mediated Shh signaling inhibition (*$P<0.006$; *$n$=7 and 4, respectively), indicating that Shh signal acts as a pro-proliferative factor on these epithelial progenitors.

Together, these data show that Shh signaling promotes, within the myotome, terminal differentiation of both epaxial and hypaxial precursors derived from the DM, whereas the actual translocation of Pax7+ precursors from the DM into myotome is Shh independent (see also Fig. 1P). They also suggest that Shh is required for maintaining proliferation of DM progenitors. Hence, Shh exerts differential effects on proliferation and differentiation in DM and myotome, respectively.

### Shh traverses the sclerotome to regulate DM-derived myogenesis

Because the notochord and floor plate appear to be the sole sources of Shh at the time of DM-derived myogenesis, we assumed that Shh molecules traverse the sclerotome to reach the DM/myotome. To test this, we assayed the effect of removing Shh from the avian sclerotome. To this end, Hhip was electroporated into the ventral epithelial somite that develops into sclerotome (*$n$=5; Fig. 4). This resulted in reduction of epaxial myotome size and the complete absence of the hypaxial domain compared with controls (*$n$=11; *$P<0.002$; Fig. 4A,B,J). As Shh activity can be visualized in the sclerotome of mouse embryos (Fig. 1), we examined whether this effect was indirectly mediated by Shh acting on sclerotomal cells.

To do this, Shh signaling was cell-autonomously inhibited in sclerotome by PTC$^{\Delta loop2}$, which had no effect on myotome size or integrity (*$n$=7; Fig. 4C,J), suggesting that secondary sclerotomal factors are not involved and further substantiating that Shh acts directly on DM/myotome (see also Fig. 3I-T).

We next tested whether the amount and/or the duration of Shh signaling was crucial for its interpretation by progenitor cells (Ahn and Joyner, 2004; Dessaud et al., 2007; Harfe et al., 2004; Ribes et al., 2010), by overexpressing Hhip in the sclerotome for either 24 hours (*$n$=6) or 16 hours (*$n$=4). We electroporated TRE-Hhip+rtTA2s-M2 in embryos that were soaked with doxycycline either immediately or 8 hours later. Myotomal area was negatively correlated with the duration of Hhip expression within the sclerotome [50% reduction compared with 25% reduction of control size; Fig. 4D-F,J; *$P<0.02$ for comparison of E and F; *$P<0.0001$ for E compared with controls (A/D); *$P<0.004$ for F compared with controls (A/D)]. Most importantly, the data suggest that Shh signaling is continuously required for differentiation, as even late Shh deprivation produced smaller myotomes.

To assess further whether Hhip acts specifically on Shh signaling, we overexpressed Shh either in sclerotome (*$n$=5) or in ectoderm (*$n$=4) in embryos in which Hhip was electroporated within the sclerotome. The deleterious effect of Hhip on myotome size was rescued by ectopic Shh emanating from either source (*$P<0.008$ and *$P<0.002$, respectively, compared with Hhip alone), yet did not reach the size of myotomes that received only Shh (*$n$=6; *$P<0.0001$ versus control; Fig. 4G-I). Together, these results show that Shh acting on
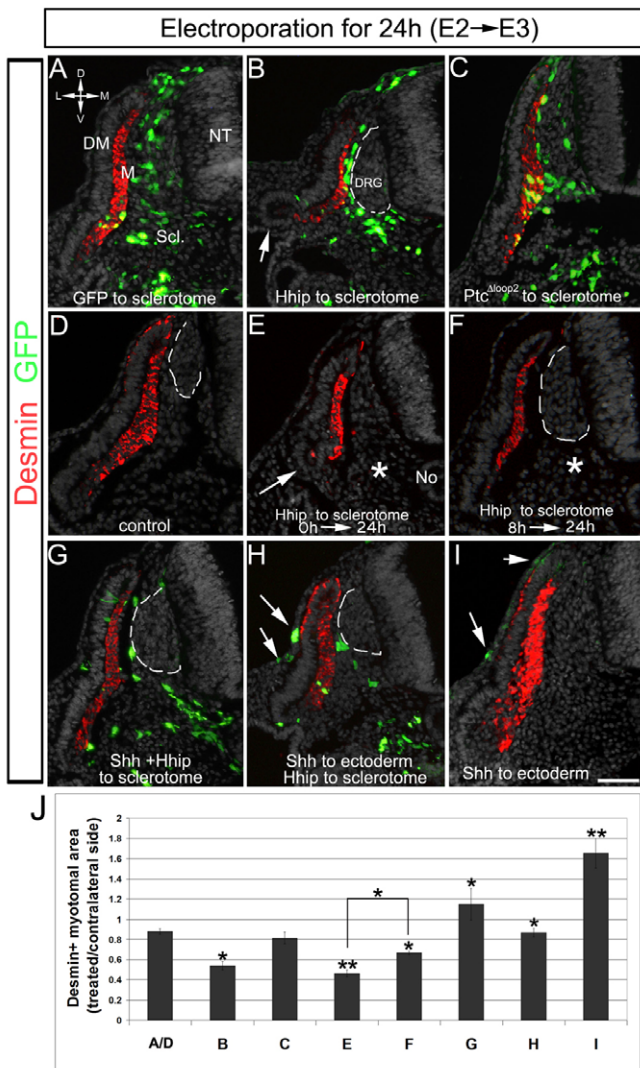
**Fig. 4. Misexpression of Hhip in avian sclerotome represses the myogenic activity of No/floor plate-derived Shh.** Transverse sections of embryos for which ventral somites were electroporated at E2 and fixed 24 hours later. (**A-F**) Control GFP (A), Hhip/GFP (B) or PTC$^{\Delta loop2}$ (C) embryos. Note in B absence of a lateral myotome with concomitant looping of the VLL (arrow). (D-F) Co-electroporation to the ventral somite (asterisk) of TRE-Hhip+rtTA2$^s$-M2 followed either by immediate activation of expression with Dox (E) or delayed activation after 8 hours (F). Note the small and intermediate sizes of the myotomes in E and F, respectively, compared with controls (A,D). The lateral myotome is virtually absent in E, as in B (arrows). (**G-I**) The effect of Hhip is rescued by excess Shh. (G) Embryos co-transfected with Shh and Hhip to sclerotome. (H) Sequential electroporation of Shh to ectoderm (arrows) followed by Hhip to sclerotome. (I) Electroporation of Shh alone to ectoderm (arrows). In addition to myotomal expression, desmin is sometimes apparent in the basal side of the medial DM (D), where it is particularly upregulated following local Shh application (H,I). (**J**) Quantification of the area occupied by desmin$^+$ myotomes in treated compared with intact contralateral sides. Letters under bars refer to treatments/groups described in A-I. Error bars represent s.e.m. *$P<0.02$, **$P<0.0001$. Dorsal root ganglia (DRG) are marked by a dashed line. Scale bar: 100 μm. DM, dermomyotome; M, myotome; NT, neural tube; Scl, sclerotome.

DM/myotome has to traverse the sclerotome, probably by forming a medial-to-lateral gradient of distribution from its midline sources towards the target sites.

## Characterization of Shh activities on myotome development in the mouse embryo
### Both activator and repressor Gli activities control mouse epaxial myotome formation

In order to address the function of Shh signaling in mouse myogenesis, we compared the spatiotemporal profile of expression of Myf5 to *Tg(GBS-GFP)* activity. Myf5 is already expressed at E9.5 at the lumbar level, before the onset of detectable Shh activity (Fig. 5A). At more rostral levels, Myf5 was induced within the entire myotome whereas the GBS-GFP activity was induced within the epaxial myotome only (Fig. 5B), This restriction of the GBS-GFP activity in mouse (Fig. 5B,H-J) contrasted with the homogeneity of Shh signaling throughout the myotome seen in avians (Figs 1, 3, 4). Importantly, in the GBS-GFP$^+$ region of the myotome, Myf5$^+$/GBS-GFP$^-$ nuclei (Fig. 5B,C) and Myf5$^+$/myosin$^+$/GBS-GFP$^-$ myocytes (Fig. 5C-C$'''$) were observed. This indicates that initial Myf5 expression might be insensitive to Gli activator signaling, and that throughout myotome development, there is likely to be a myogenic differentiation pathway independent of positive Shh activity.

To test this hypothesis, we next assessed the fate of Myf5-expressing cells in the absence of Shh. In *Shh* mutants, the loss of GBS-GFP myotomal activity and the partial death of DM progenitors (Fig. 1O-P$'$) were followed by the disappearance of the epaxial but not the hypaxial myotome (Fig. 5H-M). Thus, hypaxial myotome differentiation does not rely on Shh signaling. In addition, a Myf5$^+$ epaxial myotome was partially rescued in *Shh$^{-/-}$;Gli3$^{-/-}$* embryos, which did not display myotomal GBS-GFP activity (Fig. 5N-P). These data provide further support for the existence of two Myf5$^+$ epaxial populations, one that depends on net positive Gli activity and the other on the removal of Gli3-dependent inhibition of Shh signaling. Consistent with Gli3 repressor activity operating within the myotome, precocious upregulation of GBS-GFP was observed in *Gli3$^{-/-}$* embryos (Fig. 5D,E) (McDermott et al., 2005). A day later, at E10.5, the normal medial-to-lateral gradient of Gli activity within this tissue was not seen in *Gli3* mutants. Instead, these embryos exhibited persistent GBS-GFP activity in the lateral, more mature domain of the myotome, where GFP$^+$ cells co-expressed Arx (Fig. 5F,G). Hence, the normal shut-off of Shh signaling activity is perturbed in the absence of Gli3, suggesting that during ongoing myogenesis, Gli3 negatively modulates Shh activity. In addition, cell death was prevented in the early DM (E9.5) of the *Shh-Gli3* double mutants compared with *Shh$^{-/-}$* embryos (supplementary material Fig. S2), suggesting that Shh acts on the DM epithelium by relieving a Gli3-mediated repressor activity.

## Loss of sensitivity to Shh in the avian embryo is associated with the transition from myotome differentiation into growth
### Notochord and Shh promote myocyte differentiation at the early but not late DM stage

Analysis of the *Tg(GBS-GFP)* mice revealed that activator Shh/Gli signaling in the myotome is transient and its downregulation coincides with the appearance of Pax7$^+$ cells throughout the myotome (Fig. 2E), as opposed to earlier stages where the Pax7$^+$ cells co-expressed GBS-GFP and were restricted to the medial domain (Fig. 2B$''$), where myogenic differentiation is underway. Likewise, starting at E3 in the chick, production of differentiated myocytes diminishes and the myotome is invaded by cells that remain as Pax7$^+$ progenitors. Because Shh promotes myogenic differentiation (Figs 3, 4), we investigated whether the transition of
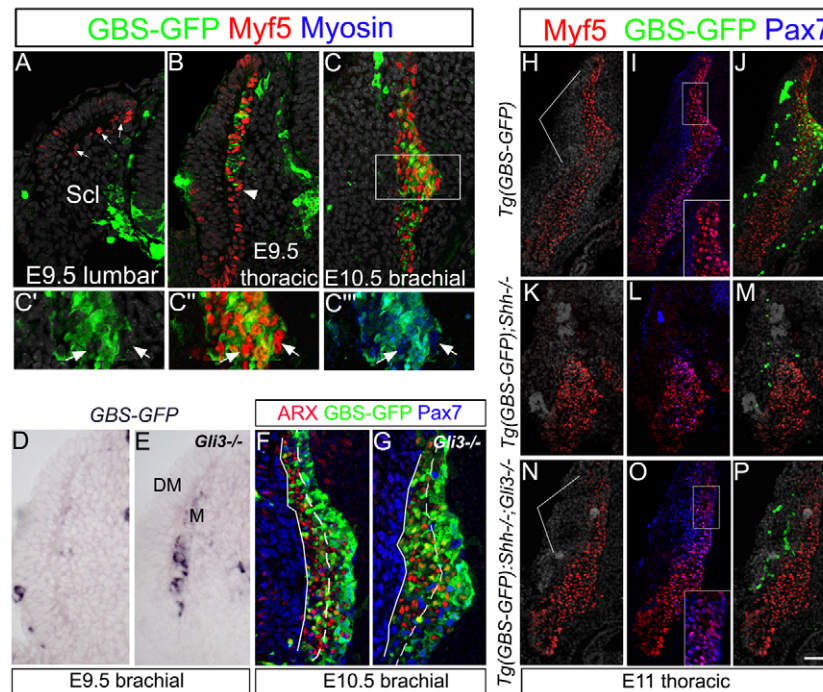
**Fig. 5. Relative contribution of Gli activator and Gli3 repressor activities to the mouse epaxial myotome developmental.** (**A-C**) Expression of Myf5, myosin and GFP in E9.5 and E10.5 *Tg(GBS-GFP)* embryos at indicated axial levels. Myf5 in myotome appears before GBS-GFP (A, arrows). GBS-GFP activity is restricted to the epaxial myotome (B; arrowhead delimits epaxial/hypaxial boundary). (**C-C‴**) Magnifications of the box in C. In the epaxial myotome, $Myf5^+/myosin^+/GBS\text{-}GFP^-$ myocytes are found (arrows). (**D,E**) ISH for *GFP* in E9.5 *Tg(GBS-GFP)* control and $Gli3^{-/-}$ embryos. The levels of *GFP* transcripts in *Gli3* mutant myotome are higher than in controls. (**F,G**) GBS-GFP, Pax7 and Arx expression in E10.5 *Tg(GBS-GFP)* and *Tg(GBS-GFP);Gli3*$^{-/-}$ embryos. Dashed lines separate medial and lateral parts of the myotome and unbroken line marks the border between myotome and dermis. In *Gli3* mutants, GBS-GFP activity persists longer and is found within the lateral myotome. (**H-P**) Expression of Myf5, Pax7 and GFP in E11.0 control, $Shh^{-/-}$ and $Shh^{-/-}; Gli3^{-/-}$ embryos all carrying *Tg(GBS-GFP)*. Insets in O and I are magnifications of boxes in main panels. Both $Shh^{-/-}$ and $Shh^{-/-}; Gli3^{-/-}$ embryos lack myotomal GBS-GFP activity; remaining $GFP^+$ cells are blood cells. Yet, lack of *Gli3* rescues the reduction of $Myf5^+$ epaxial myotome in absence of *Shh* function. Lines in H and N demarcate the epaxial myotome. All pictures are transverse sections. DM, dermomyotome, M, myotome, Scl, sclerotome. Scale bar: in A-C,F,G, 50 μm; in D,E, 40 μm; in H-P, 125 μm.

the DM from differentiation to growth was triggered by a lack of sufficient Shh signal reaching this tissue or from cells becoming refractory to the ligand. To discriminate between these possibilities, we adopted a gain-of-function approach in the chick. Notochord fragments were grafted dorsal to the epithelial somite or DM at E2 or E3, respectively. A dramatic stimulation of myogenesis occurred a day later in the early-stage implants with massive differentiation into desmin$^+$ myocytes at the expense of Pax7$^+$ DM progenitors (*n*=10; Fig. 6A,B). By contrast, no effect on myogenesis was observed upon late grafting as desmin$^+$ myocytes and Pax7$^+$ progenitors were similarly distributed in treated versus contralateral myotomes (*n*=7; Fig. 6C-D′). Likewise, electroporation of Shh to the ectoderm at E2 promoted myogenic differentiation at the expense of Pax7$^+$ progenitors (Fig. 6E-F′), a phenotype reciprocal to that observed upon Shh inhibition in both species (Figs 1, 3). Moreover, dermis development was prevented and, instead, the epithelial structure of the DM was maintained but adopted an undulated form compared with the contralateral side in which the central DM has already dissociated to generate dermis and Pax7$^+$ myotomal progenitors (*n*=10; Fig. 6E,F). This suggests that Shh affects both maintenance of DM epithelial character and proliferation, in agreement with results of loss of Shh function (Fig. 3). In striking contrast, late Shh misexpression had no apparent effect on muscle or dermis development, consistent with results of the late notochord grafts (*n*=12; Fig. 6G-H′). The observed lack of

effect of the late procedures cannot be explained by the target cells being further away from Shh sources at E3, because at this time the dermis is yet to form (see Fig. 6A), and late notochord grafts or Shh-transfected ectoderm were as closely apposed to the targets as they were at E2. Together, this excludes the possibility that, under normal conditions, lack of responsiveness is accounted for by tissue growth, which might result in insufficient Shh reaching the target DM/myotome from midline sources. Hence, both loss- and gain-of-function data demonstrate that Shh is myogenic to the dorsal somite and early DM, but that the late DM becomes refractory.

### The block to Shh responsiveness lies at the level of or upstream of Smo signaling

To determine more precisely the level at which the lack of responsiveness of DM/myotome cells to Shh occurs, we attempted to rescue myogenic differentiation at various levels of the Shh-dependent pathway. To this end, we electroporated MyoD, which is induced by Shh signaling (Kahane et al., 2001), an active form of Gli (GliA) or constitutively active Smo (SmoM2) into the late DM at E3 and compared their effects to early-stage electroporations (E2). In all controls, GFP-labeled cells were observed in both dermis and myotome (*n*=30; Fig. 7A,B,I,J; supplementary material Fig. S3A,E). Within the myotome of early GFP-transfected embryos, cells were either Pax7$^+$ progenitors or desmin$^+$/Pax7$^-$ fibers (*n*=11; Fig. 7A,B) (supplementary material Fig. S3A,A′). By
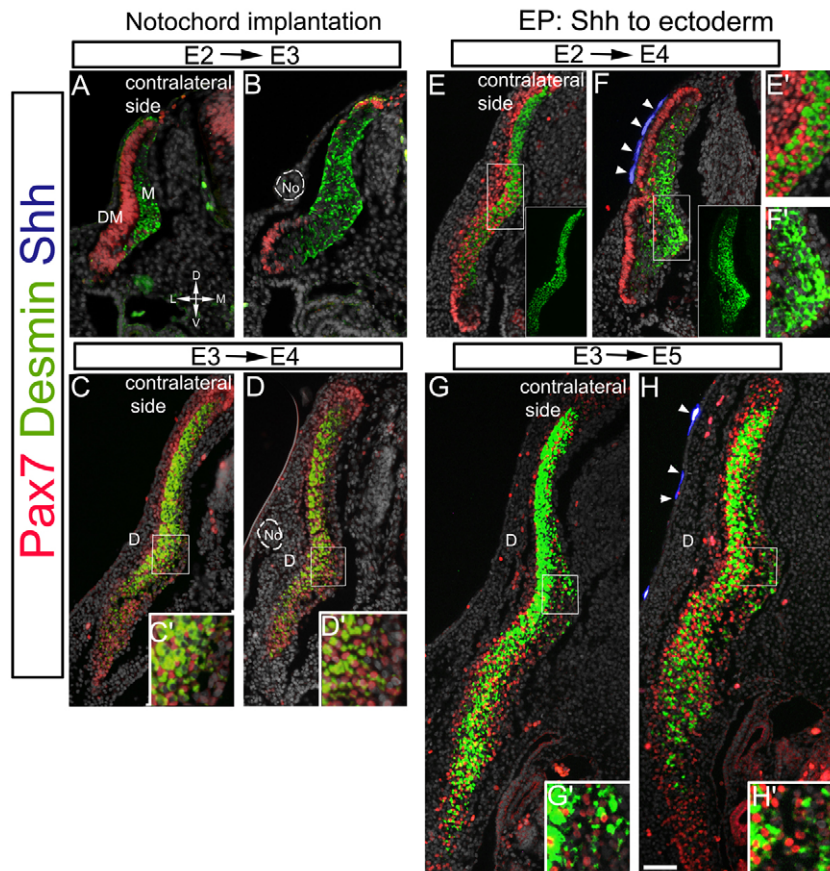
**Fig. 6. Avian myotome development transits from a Shh-dependent to a Shh-refractory phase.**
(**A-D**) Grafting of a No fragment dorsal to the young somite (A,B), or the late DM (C,D). (**E-H**) Co-electroporation of Shh-GFP to the ectoderm (blue, arrowheads) of E2 (E,F) or E3 (G,H) embryos. Insets in E,F show desmin staining only. (**C′,D′,E′,F′,G′,H′**) Higher magnifications of respective boxed areas. Myotome differentiation in response to No or *Shh* is time restricted. D, dermis; DM, dermomyotome; M, myotome. Scale bar: in A,B, 85 μm; in C-H, 100 μm.

contrast, in late electroporations, most control cells were Pax7^{+} and the DM no longer generated fibers (*n*=10; Fig. 7I,J; supplementary material Fig. S3E,E′) (Ben-Yair and Kalcheim, 2005). All three plasmids examined promoted myogenic differentiation at the expense of Pax7^{+} progenitors in the myotome at both the early and late DM stages, and also at the expense of dermis at the early stage only (*n*=7, 15 and 8 for early treatments with MyoD, GliA and SmoM2, respectively; *n*=5, 12 and 10 for equivalent treatments at the late stage; *P*<0.001 for MyoD versus control and *P*<0.0001 for all other treatments; Fig. 7C-Q; supplementary material Fig. S3). This was in stark contrast to Shh and notochord grafts that stimulated myogenesis at the early but not later time points (Fig. 6). Thus, downstream components of the Shh signaling pathway are able to rescue myogenesis in the mature DM, which is insensitive to Shh, indicating that the lack of responsiveness to Shh is most likely to lie at the level of or upstream of Smo signaling.

## DISCUSSION
In the light of our data, we propose a model in which the dynamics of Shh signaling within the DM and myotome are essential to establish key transitions in the development of skeletal muscle. We demonstrate that the myogenic role of Shh is regulated in both space and time, thus accounting for the transition from an early differentiation phase to a subsequent growth phase of the muscle primordium. Furthermore, comparisons between both species revealed striking similarities but also differences in cellular and molecular events underlying myotome development.

Using *Tg(GBS-GFP)* mice as a reporter of Shh-dependent Gli activity, we provide evidence of a decreasing medial-to-lateral gradient of Shh activity in the sclerotome. A similar gradient is

formed in the ventral neural tube (Balaskas et al., 2012; Chamberlain et al., 2008), which subdivides this territory into different neuronal precursor domains (Jessell, 2000). Importantly, Shh signaling decreases within this tissue at the time the myotome starts differentiating. The subsequent decrease in *Hhip* and *Ptc1* expression, which can both sequester Shh ligand, is probably a prerequisite for the morphogen to be able to traverse the sclerotome and reach the myotome. Evidence that Shh traversing the sclerotome is of functional significance for myogenesis stems from avians in which Shh was locally titrated out with Hhip, resulting in compromised myotomes. Further consolidation of such a gradient could be provided by the observed counter-gradient of *Gli3* production apparent in the chick sclerotome (Fig. 1).

In spite of the low GBS-GFP signal levels in the dorsal sclerotome, strong GBS-GFP activity was detected in the adjacent myotome. This cannot be accounted for by the concentration gradient of Shh alone and suggests that local regulatory activities modulate Shh function. *Gli1* and *Gli2*, *Sulf1*, *Hhip*, *Cdo* and *Ptc1* are transcribed in myotome whereas *Gli1*, *Gli2*, *Gli3*, *Boc*, *Gas* and *Cdo* are expressed in DM. Cdo, Boc and Gas enhance Shh signaling but are transcriptionally downregulated by the ligand. Conversely, Ptc1 and Hhip inhibit Shh signaling yet are transcriptionally upregulated, providing negative-feedback control (Ribes and Briscoe, 2009). Thus, an integration of positive and negative components of the pathway imparted by these and perhaps additional modulators is likely to provide such a local regulation.

Our gain- and loss-of-function data show that Shh also modulates cell proliferation and the maintenance of epithelial characteristics in the avian DM. However, GBS-GFP activity is not detected in the mouse DM. Several possibilities could account for this observation.
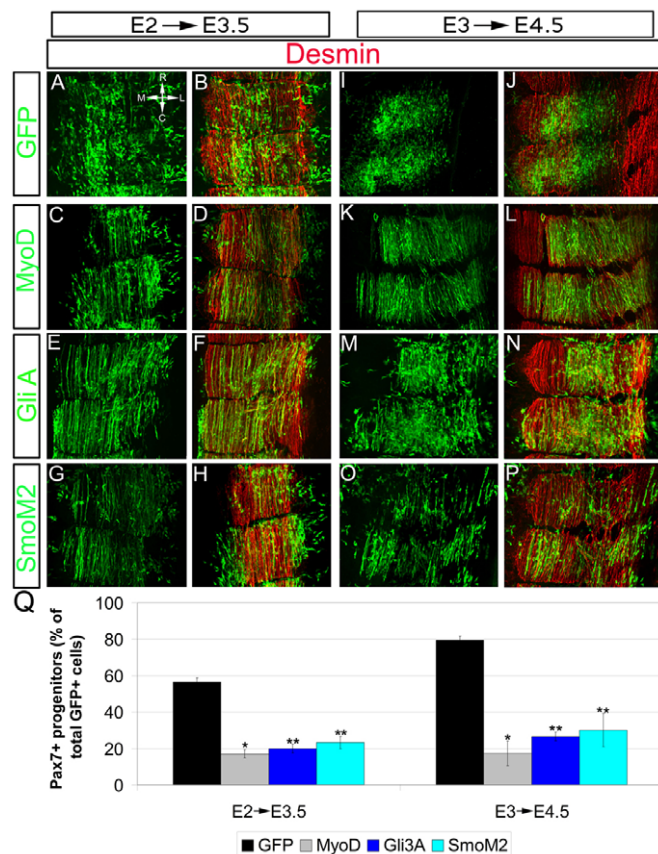
**Fig. 7. DM progenitors, although refractory to Shh ligand, respond to Shh signaling components acting at the level of or downstream of Smo.** (**A-P**) Dorsal views of whole-mount preparations at E3.5 (A-H) and E4.5 (I-J) labeled for GFP and desmin. Control-GFP (A,B,I,J), MyoD (C,D,K,L), GliA (E,F,M,N) or SmoM2 (G,H,O,P) were electroporated within dorsal somites at E2 (A-H) or DM at E3 (I-P). All the components of Shh signaling enhanced DM-derived myogenic differentiation compared with control-GFP. Note that, at E3, control-GFP does not generate myofibers. (**Q**) Quantification of the proportion of Pax7+ progenitors in myotome. Error bars represent s.e.m. *$P<0.001$, **$P<0.0001$.

First, GBS-GFP activity in DM could be below the detectable threshold, a notion consistent with *in vitro* data suggesting that the lowest level of Shh signaling allows DM gene expression (Cairns et al., 2008). Alternatively, Shh might signal the DM by removing a Gli3-mediated repressor activity, as cell death observed in the DM of Shh$^{-/-}$ embryos was prevented in *Shh-Gli3* compound mutants. The possibility also remains open that the mouse DM responds to Shh via a Gli-independent non-canonical pathway (Polizio et al., 2011).

It was previously shown that avian myotome development involves three stages (Kalcheim and Ben-Yair, 2005). A first wave of pioneer myoblasts originating from the medial somite, a second wave from the lips and central sheet of the DM and a third wave from the dissociating central DM. Whereas the first and second waves generate differentiated myocytes, the last wave produces Pax7+ mitotic progenitors that account for myotome growth. Our data indicate that second-wave progenitors emanating from the DM depend upon Shh for terminal differentiation. By contrast, the third wave is refractory to this factor.

In mouse, we find that Shh signaling also has a differential role during both the patterning and the growth phases. Analysis of *Tg(GBS-GFP)* mice in conjunction with *Shh* and *Gli3* mutants during the patterning phase provides evidence that two myogenic subpopulations co-exist in the epaxial myotome. First, myoblasts expressing Myf5 but devoid of GBS-GFP, are observed from the earliest stage of myogenesis. Because these myoblasts terminally differentiate, we suggest that their development is independent of positive Shh signaling. In addition, a second subpopulation is characterized by high levels of GBS-GFP activity. Because in *Shh* mutants there is no epaxial myotome (Fig. 5) (Borycki et al., 1999), it is conceivable that both GBS-GFP-positive and GBS-GFP-negative cells require Shh for survival. We then postulated that the GBS-GFP-negative subpopulation depends on relief of inhibition conveyed by Gli3. As there is a significant rescue of the epaxial component in compound *Gli3* and *Shh* mutants, we conclude that, in addition to positive signaling, a negative regulation of cell survival and myogenesis is imparted by Gli3 in the absence of Shh. Finally, during the growth phase, identified by the large number of Pax7+ progenitors spread throughout the myotome, GBS-GFP and transcription of direct Shh target genes are downregulated. Moreover, the number of Pax7+ cells remains unaltered in the absence of Gli3, marking the end of both positive and negative Shh signaling in myotome. This indicates that, similar to the chick, the role of Shh is transient and ends when the myotome transits from a differentiation phase into a growth phase.

Differential activity of Shh on the epaxial versus hypaxial myotome also became evident from analysis of *Tg(GBS-GFP)* embryos, in which GBS-GFP activity was restricted to the epaxial domain. Hypaxial progenitors seem to be insensitive to either positive and/or negative Shh activities as the hypaxial myotome was unaffected in *Shh* mutants at E11.5 (Fig. 5). By contrast, data from *Xenopus* (Martin et al., 2007) as well as from avians (Figs 3, 4) suggest that both domains are receptive. Differential responsiveness to Shh with regard to timing, ligand concentrations and distribution of distinct pathway components has also been reported in zebrafish (Buckingham and Vincent, 2009; Lewis et al., 1999; Wolff et al., 2003). Altogether, it is conceivable that from zebrafish to rodents, a number of growth factor combinations that include Shh have been used differently to form muscles. This complexity might reflect the existence of a vertebrate ancestral mechanism that involves the differential use of distinct cell subsets.

Analysis of the dynamics of combinatorial marker expression in conjunction with GBS-GFP activity reveals that there is a spatial and temporal order of myotome development in the mouse that resembles the patterns reported in avian embryos. Birthdating analysis (Kahane et al., 1998b) as well as GFP marking of pioneer myoblasts (Fig. 2F) in the chick showed that the myotome matures in a lateral to medial direction. Notably, Shh activity is mainly detected in the differentiating medial region and is lost in the lateral domain where markers of terminal differentiation are apparent (Arx, myosin), further substantiating the notion that Shh is necessary for a specific phase of myoblast differentiation. This mediolateral order of maturation is lost in *Gli3* mutants. Hence, the end of Shh activity is accounted for, at least partially, by a negative Gli3 input that is responsible for regulating signal duration but has no apparent effect on actual cell differentiation.

Similar to the mouse data, a transition from an initial Shh-dependent phase into a later refractory phase was observed in avians. This transition cannot be accounted for by the increasing size of the embryo and consequent lack of sufficient Shh, as late application of either a notochord graft or of Shh close to the DM/myotome were ineffective in stimulating myogenesis. However, misexpression of downstream components of the Shh

pathway (MyoD and activated forms of Gli and Smo) in the mature DM rescued myogenesis. This might indicate that the advent of insensitivity to Shh is at the level of or upstream of Smo signaling. Analogous to the DM/myotome, a decrease in sensitivity of floorplate cells to Shh signaling was documented (Cruz et al., 2010; Ribes et al., 2010); FoxA2 is likely to mediate this effect partly by inhibiting expression of Shh pathway components downstream of Smo (Ribes et al., 2010). In the DM, one possible event that coincides in time with loss of Shh responsiveness is its conversion into mesenchyme, during which production of myotomal fibers is substituted by mitotic Pax7$^+$ progenitors that are Shh-insensitive in both mice and avians. DM dissociation is triggered by myotomal fibroblast growth factor signaling (Delfini et al., 2009), and by loss of N-cadherin (cadherin 2), which also alters their apicobasal polarity (Ben-Yair et al., 2011; Cinnamon et al., 2006); the processes described above could alter the composition or organization of cilia responsible for signal transduction (Eggenschwiler and Anderson, 2007). Along this line, apically aligned cilia present in the epithelial DM change their distribution upon DM dissociation to become randomly localized on the cell surface (our unpublished data). Whether these processes are functionally coupled to the loss of responsiveness to Shh and concomitant transition from differentiation into growth remains to be elucidated.

### Competing interests statement
The authors declare no competing financial interests.

### Supplementary material
Supplementary material available online at
http://dev.biologists.org/lookup/suppl/doi:10.1242/dev.092726/-/DC1

### References
**Ahn, S. and Joyner, A. L.** (2004). Dynamic changes in the response of cells to positive hedgehog signaling during mouse limb patterning. *Cell* **118**, 505-516.
**Allen, B. L., Song, J. Y., Izzi, L., Althaus, I. W., Kang, J. S., Charron, F., Krauss, R. S. and McMahon, A. P.** (2011). Overlapping roles and collective requirement for the coreceptors GAS1, CDO, and BOC in SHH pathway function. *Dev. Cell* **20**, 775-787.
**Amthor, H., Christ, B. and Patel, K.** (1999). A molecular mechanism enabling continuous embryonic muscle growth – a balance between proliferation and differentiation. *Development* **126**, 1041-1053.
**Anderson, C., Williams, V. C., Moyon, B., Daubas, P., Tajbakhsh, S., Buckingham, M. E., Shiroishi, T., Hughes, S. M. and Borycki, A. G.** (2012). Sonic hedgehog acts cell-autonomously on muscle precursor cells to generate limb muscle diversity. *Genes Dev.* **26**, 2103-2117.
**Balaskas, N., Ribeiro, A., Panovska, J., Dessaud, E., Sasai, N., Page, K. M., Briscoe, J. and Ribes, V.** (2012). Gene regulatory logic for reading the Sonic Hedgehog signaling gradient in the vertebrate neural tube. *Cell* **148**, 273-284.
**Ben-Yair, R. and Kalcheim, C.** (2005). Lineage analysis of the avian dermomyotome sheet reveals the existence of single cells with both dermal and muscle progenitor fates. *Development* **132**, 689-701.
**Ben-Yair, R. and Kalcheim, C.** (2008). Notch and bone morphogenetic protein differentially act on dermomyotome cells to generate endothelium, smooth, and striated muscle. *J. Cell Biol.* **180**, 607-618.
**Ben-Yair, R., Kahane, N. and Kalcheim, C.** (2011). LGN-dependent orientation of cell divisions in the dermomyotome controls lineage segregation into muscle and dermis. *Development* **138**, 4155-4166.
**Biressi, S., Messina, G., Collombat, P., Tagliafico, E., Monteverde, S., Benedetti, L., Cusella De Angelis, M. G., Mansouri, A., Ferrari, S.,**

**Tajbakhsh, S. et al.** (2008). The homeobox gene Arx is a novel positive regulator of embryonic myogenesis. *Cell Death Differ.* **15**, 94-104.
**Blagden, C. S. and Hughes, S. M.** (1999). Extrinsic influences on limb muscle organisation. *Cell Tissue Res.* **296**, 141-150.
**Boardman, P. E., Sanz-Ezquerro, J., Overton, I. M., Burt, D. W., Bosch, E., Fong, W. T., Tickle, C., Brown, W. R., Wilson, S. A. and Hubbard, S. J.** (2002). A comprehensive collection of chicken cDNAs. *Curr. Biol.* **12**, 1965-1969.
**Borycki, A. G., Mendham, L. and Emerson, C. P., Jr** (1998). Control of somite patterning by Sonic hedgehog and its downstream signal response genes. *Development* **125**, 777-790.
**Borycki, A. G., Brunk, B., Tajbakhsh, S., Buckingham, M., Chiang, C. and Emerson, C. P., Jr** (1999). Sonic hedgehog controls epaxial muscle determination through Myf5 activation. *Development* **126**, 4053-4063.
**Briscoe, J., Chen, Y., Jessell, T. M. and Struhl, G.** (2001). A hedgehog-insensitive form of patched provides evidence for direct long-range morphogen activity of sonic hedgehog in the neural tube. *Mol. Cell* **7**, 1279-1291.
**Buckingham, M.** (2001). Skeletal muscle formation in vertebrates. *Curr. Opin. Genet. Dev.* **11**, 440-448.
**Buckingham, M. and Montarras, D.** (2008). Skeletal muscle stem cells. *Curr. Opin. Genet. Dev.* **18**, 330-336.
**Buckingham, M. and Vincent, S. D.** (2009). Distinct and dynamic myogenic populations in the vertebrate embryo. *Curr. Opin. Genet. Dev.* **19**, 444-453.
**Büscher, D., Grotewold, L. and Rüther, U.** (1998). The XtJ allele generates a Gli3 fusion transcript. *Mamm. Genome* **9**, 676-678.
**Buttitta, L., Mo, R., Hui, C. C. and Fan, C. M.** (2003). Interplays of Gli2 and Gli3 and their requirement in mediating Shh-dependent sclerotome induction. *Development* **130**, 6233-6243.
**Cairns, D. M., Sato, M. E., Lee, P. G., Lassar, A. B. and Zeng, L.** (2008). A gradient of Shh establishes mutually repressing somitic cell fates induced by Nkx3.2 and Pax3. *Dev. Biol.* **323**, 152-165.
**Chamberlain, C. E., Jeong, J., Guo, C., Allen, B. L. and McMahon, A. P.** (2008). Notochord-derived Shh concentrates in close association with the apically positioned basal body in neural target cells and forms a dynamic gradient during neural patterning. *Development* **135**, 1097-1106.
**Charrier, J. B., Lapointe, F., Le Douarin, N. M. and Teillet, M. A.** (2001). Anti-apoptotic role of Sonic hedgehog protein at the early stages of nervous system organogenesis. *Development* **128**, 4011-4020.
**Chiang, C., Litingtung, Y., Lee, E., Young, K. E., Corden, J. L., Westphal, H. and Beachy, P. A.** (1996). Cyclopia and defective axial patterning in mice lacking Sonic hedgehog gene function. *Nature* **383**, 407-413.
**Christ, B. and Scaal, M.** (2008). Formation and differentiation of avian somite derivatives. *Adv. Exp. Med. Biol.* **638**, 1-41.
**Chuang, P. T. and McMahon, A. P.** (1999). Vertebrate Hedgehog signalling modulated by induction of a Hedgehog-binding protein. *Nature* **397**, 617-621.
**Cinnamon, Y., Kahane, N. and Kalcheim, C.** (1999). Characterization of the early development of specific hypaxial muscles from the ventrolateral myotome. *Development* **126**, 4305-4315.
**Cinnamon, Y., Kahane, N., Bachelet, I. and Kalcheim, C.** (2001). The sub-lip domain – a distinct pathway for myotome precursors that demonstrate rostral-caudal migration. *Development* **128**, 341-351.
**Cinnamon, Y., Ben-Yair, R. and Kalcheim, C.** (2006). Differential effects of N-cadherin-mediated adhesion on the development of myotomal waves. *Development* **133**, 1101-1112.
**Cruz, C., Ribes, V., Kutejova, E., Cayuso, J., Lawson, V., Norris, D., Stevens, J., Davey, M., Blight, K., Bangs, F. et al.** (2010). Foxj1 regulates floor plate cilia architecture and modifies the response of cells to sonic hedgehog signalling. *Development* **137**, 4271-4282.
**Danesin, C., Agius, E., Escalas, N., Ai, X., Emerson, C., Cochard, P. and Soula, C.** (2006). Ventral neural progenitors switch toward an oligodendroglial fate in response to increased Sonic hedgehog (Shh) activity: involvement of Sulfatase 1 in modulating Shh signaling in the ventral spinal cord. *J. Neurosci.* **26**, 5037-5048.
**Delfini, M. C. and Duprez, D.** (2004). Ectopic Myf5 or MyoD prevents the neuronal differentiation program in addition to inducing skeletal muscle differentiation, in the chick neural tube. *Development* **131**, 713-723.
**Delfini, M. C., De La Celle, M., Gros, J., Serralbo, O., Marics, I., Seux, M., Scaal, M. and Marcelle, C.** (2009). The timing of emergence of muscle progenitors is controlled by an FGF/ERK/SNAIL1 pathway. *Dev. Biol.* **333**, 229-237.
**Dessaud, E., Yang, L. L., Hill, K., Cox, B., Ulloa, F., Ribeiro, A., Mynett, A., Novitch, B. G. and Briscoe, J.** (2007). Interpretation of the sonic hedgehog morphogen gradient by a temporal adaptation mechanism. *Nature* **450**, 717-720.
**Devoto, S. H., Stoiber, W., Hammond, C. L., Steinbacher, P., Haslett, J. R., Barresi, M. J., Patterson, S. E., Adiarte, E. G. and Hughes, S. M.** (2006). Generality of vertebrate developmental patterns: evidence for a dermomyotome in fish. *Evol. Dev.* **8**, 101-110.

Dhoot, G. K., Gustafsson, M. K., Ai, X., Sun, W., Standiford, D. M. and Emerson, C. P., Jr (2001). Regulation of Wnt signaling and embryo patterning by an extracellular sulfatase. *Science* **293**, 1663-1666.

Du, S. J., Devoto, S. H., Westerfield, M. and Moon, R. T. (1997). Positive and negative regulation of muscle cell identity by members of the hedgehog and TGF-beta gene families. *J. Cell Biol.* **139**, 145-156.

Eggenschwiler, J. T. and Anderson, K. V. (2007). Cilia and developmental signaling. *Annu. Rev. Cell Dev. Biol.* **23**, 345-373.

Feng, X., Adiarte, E. G. and Devoto, S. H. (2006). Hedgehog acts directly on the zebrafish dermomyotome to promote myogenic differentiation. *Dev. Biol.* **300**, 736-746.

Gros, J., Scaal, M. and Marcelle, C. (2004). A two-step mechanism for myotome formation in chick. *Dev. Cell* **6**, 875-882.

Gros, J., Manceau, M., Thomé, V. and Marcelle, C. (2005). A common somitic origin for embryonic muscle progenitors and satellite cells. *Nature* **435**, 954-958.

Groysman, M., Shoval, I. and Kalcheim, C. (2008). A negative modulatory role for rho and rho-associated kinase signaling in delamination of neural crest cells. *Neural Dev.* **3**, 27.

Gustafsson, M. K., Pan, H., Pinney, D. F., Liu, Y. L., Lewandowski, A., Epstein, D. J. and Emerson, C. P., Jr (2002). Myf5 is a direct target of long-range Shh signaling and Gli regulation for muscle specification. *Genes Dev.* **16**, 114-126.

Halperin-Barlev, O. and Kalcheim, C. (2011). Sclerotome-derived Slit1 drives directional migration and differentiation of Robo2-expressing pioneer myoblasts. *Development* **138**, 2935-2945.

Hammond, C. L., Hinits, Y., Osborn, D. P., Minchin, J. E., Tettamanti, G. and Hughes, S. M. (2007). Signals and myogenic regulatory factors restrict pax3 and pax7 expression to dermomyotome-like tissue in zebrafish. *Dev. Biol.* **302**, 504-521.

Harfe, B. D., Scherz, P. J., Nissim, S., Tian, H., McMahon, A. P. and Tabin, C. J. (2004). Evidence for an expansion-based temporal Shh gradient in specifying vertebrate digit identities. *Cell* **118**, 517-528.

Hu, J. K., McGlinn, E., Harfe, B. D., Kardon, G. and Tabin, C. J. (2012). Autonomous and nonautonomous roles of Hedgehog signaling in regulating limb muscle formation. *Genes Dev.* **26**, 2088-2102.

Huang, R. and Christ, B. (2000). Origin of the epaxial and hypaxial myotome in avian embryos. *Anat. Embryol. (Berl.)* **202**, 369-374.

Hui, C. C. and Joyner, A. L. (1993). A mouse model of greig cephalopolysyndactyly syndrome: the extra-toesJ mutation contains an intragenic deletion of the Gli3 gene. *Nat. Genet.* **3**, 241-246.

Hynes, M., Ye, W., Wang, K., Stone, D., Murone, M., Sauvage, F. and Rosenthal, A. (2000). The seven-transmembrane receptor smoothened cell-autonomously induces multiple ventral cell types. *Nat. Neurosci.* **3**, 41-46.

Incardona, J. P., Gaffield, W., Kapur, R. P. and Roelink, H. (1998). The teratogenic Veratrum alkaloid cyclopamine inhibits sonic hedgehog signal transduction. *Development* **125**, 3553-3562.

Ingham, P. W. and McMahon, A. P. (2001). Hedgehog signaling in animal development: paradigms and principles. *Genes Dev.* **15**, 3059-3087.

Izzi, L., Lévesque, M., Morin, S., Laniel, D., Wilkes, B. C., Mille, F., Krauss, R. S., McMahon, A. P., Allen, B. L. and Charron, F. (2011). Boc and Gas1 each form distinct Shh receptor complexes with Ptch1 and are required for Shh-mediated cell proliferation. *Dev. Cell* **20**, 788-801.

Jessell, T. M. (2000). Neuronal specification in the spinal cord: inductive signals and transcriptional codes. *Nat. Rev. Genet.* **1**, 20-29.

Kahane, N., Cinnamon, Y. and Kalcheim, C. (1998a). The origin and fate of pioneer myotomal cells in the avian embryo. *Mech. Dev.* **74**, 59-73.

Kahane, N., Cinnamon, Y. and Kalcheim, C. (1998b). The cellular mechanism by which the dermomyotome contributes to the second wave of myotome development. *Development* **125**, 4259-4271.

Kahane, N., Cinnamon, Y., Bachelet, I. and Kalcheim, C. (2001). The third wave of myotome colonization by mitotically competent progenitors: regulating the balance between differentiation and proliferation during muscle development. *Development* **128**, 2187-2198.

Kahane, N., Cinnamon, Y. and Kalcheim, C. (2002). The roles of cell migration and myofiber intercalation in patterning formation of the postmitotic myotome. *Development* **129**, 2675-2687.

Kahane, N., Ben-Yair, R. and Kalcheim, C. (2007). Medial pioneer fibers pattern the morphogenesis of early myoblasts derived from the lateral somite. *Dev. Biol.* **305**, 439-450.

Kalcheim, C. and Ben-Yair, R. (2005). Cell rearrangements during development of the somite and its derivatives. *Curr. Opin. Genet. Dev.* **15**, 371-380.

Kassar-Duchossoy, L., Giacone, E., Gayraud-Morel, B., Jory, A., Gomès, D. and Tajbakhsh, S. (2005). Pax3/Pax7 mark a novel population of primitive myogenic cells during development. *Genes Dev.* **19**, 1426-1431.

Krüger, M., Mennerich, D., Fees, S., Schäfer, R., Mundlos, S. and Braun, T. (2001). Sonic hedgehog is a survival factor for hypaxial muscles during mouse development. *Development* **128**, 743-752.

Lewis, K. E., Concordet, J. P. and Ingham, P. W. (1999). Characterisation of a second patched gene in the zebrafish Danio rerio and the differential response of patched genes to Hedgehog signalling. *Dev. Biol.* **208**, 14-29.

Lewis, P. M., Dunn, M. P., McMahon, J. A., Logan, M., Martin, J. F., St-Jacques, B. and McMahon, A. P. (2001). Cholesterol modification of sonic hedgehog is required for long-range signaling activity and effective modulation of signaling by Ptc1. *Cell* **105**, 599-612.

Martin, B. L., Peyrot, S. M. and Harland, R. M. (2007). Hedgehog signaling regulates the amount of hypaxial muscle development during Xenopus myogenesis. *Dev. Biol.* **304**, 722-734.

Maurya, A. K., Tan, H., Souren, M., Wang, X., Wittbrodt, J. and Ingham, P. W. (2011). Integration of Hedgehog and BMP signalling by the engrailed2a gene in the zebrafish myotome. *Development* **138**, 755-765.

McDermott, A., Gustafsson, M., Elsam, T., Hui, C. C., Emerson, C. P., Jr and Borycki, A. G. (2005). Gli2 and Gli3 have redundant and context-dependent function in skeletal muscle formation. *Development* **132**, 345-357.

Momose, T., Tonegawa, A., Takeuchi, J., Ogawa, H., Umesono, K. and Yasuda, K. (1999). Efficient targeting of gene expression in chick embryos by microelectroporation. *Dev. Growth Differ.* **41**, 335-344.

Nitzan, E. and Kalcheim, C. (2013). Neural crest and somitic mesoderm as paradigms to investigate cell fate decisions during development. *Dev. Growth Differ.* **55**, 60-78.

Polizio, A. H., Chinchilla, P., Chen, X., Manning, D. R. and Riobo, N. A. (2011). Sonic Hedgehog activates the GTPases Rac1 and RhoA in a Gli-independent manner through coupling of smoothened to Gi proteins. *Sci. Signal.* **4**, pt7.

Pownall, M. E. and Emerson, C. P., Jr (1992). Sequential activation of three myogenic regulatory genes during somite morphogenesis in quail embryos. *Dev. Biol.* **151**, 67-79.

Relaix, F., Rocancourt, D., Mansouri, A. and Buckingham, M. (2005). A Pax3/Pax7-dependent population of skeletal muscle progenitor cells. *Nature* **435**, 948-953.

Ribes, V. and Briscoe, J. (2009). Establishing and interpreting graded Sonic Hedgehog signaling during vertebrate neural tube patterning: the role of negative feedback. *Cold Spring Harb. Perspect. Biol.* **1**, a002014.

Ribes, V., Balaskas, N., Sasai, N., Cruz, C., Dessaud, E., Cayuso, J., Tozer, S., Yang, L. L., Novitch, B., Marti, E. et al. (2010). Distinct Sonic Hedgehog signaling dynamics specify floor plate and ventral neuronal progenitors in the vertebrate neural tube. *Genes Dev.* **24**, 1186-1200.

Sasaki, H., Hui, C., Nakafuku, M. and Kondoh, H. (1997). A binding site for Gli proteins is essential for HNF-3beta floor plate enhancer activity in transgenics and can respond to Shh in vitro. *Development* **124**, 1313-1322.

Scaal, M. and Christ, B. (2004). Formation and differentiation of the avian dermomyotome. *Anat. Embryol. (Berl.)* **208**, 411-424.

Stamataki, D., Ulloa, F., Tsoni, S. V., Mynett, A. and Briscoe, J. (2005). A gradient of Gli activity mediates graded Sonic Hedgehog signaling in the neural tube. *Genes Dev.* **19**, 626-641.

Stellabotte, F. and Devoto, S. H. (2007). The teleost dermomyotome. *Dev. Dyn.* **236**, 2432-2443.

Teboul, L., Summerbell, D. and Rigby, P. W. (2003). The initial somitic phase of Myf5 expression requires neither Shh signaling nor Gli regulation. *Genes Dev.* **17**, 2870-2874.

Teillet, M. A., Lapointe, F. and Le Douarin, N. M. (1998). The relationships between notochord and floor plate in vertebrate development revisited. *Proc. Natl. Acad. Sci. USA* **95**, 11733-11738.

Watanabe, T., Saito, D., Tanabe, K., Suetsugu, R., Nakaya, Y., Nakagawa, S. and Takahashi, Y. (2007). Tet-on inducible system combined with in ovo electroporation dissects multiple roles of genes in somitogenesis of chicken embryos. *Dev. Biol.* **305**, 625-636.

Wolff, C., Roy, S. and Ingham, P. W. (2003). Multiple muscle cell identities induced by distinct levels and timing of hedgehog activity in the zebrafish embryo. *Curr. Biol.* **13**, 1169-1181.
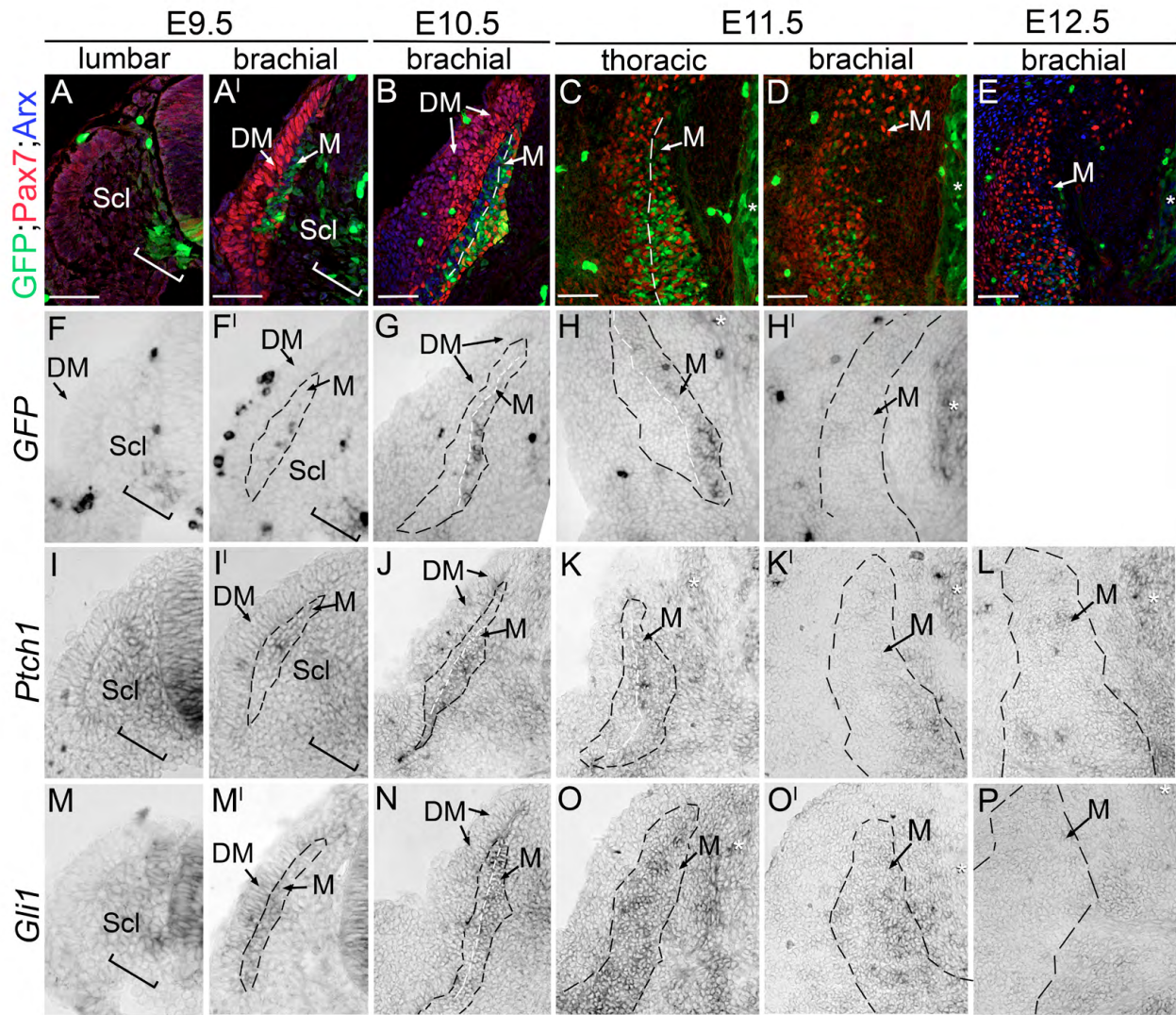
**Fig. S1. Dynamics of Gli activity in myotome and sclerotome of mouse embryos.** (**A-P**) Immunostaining for Pax7, GFP (A-E) and Arx (A,B,E), and ISH for *GFP* (F-H'), *Ptch1* (I-L) or *Gli1* (M-P) on transverse sections of *Tg(GBS-GFP)* mouse embryos at the indicated stage and axial levels. All the markers show that the myotome presents transient high levels of Shh signaling. The expression of GFP protein and mRNA driven by the 8xGBS enhancer is detected in the forming myotome from E9.5 in brachial regions of the embryos (A',F'). As more myotomal cells differentiate, the expression of the reporter of Gli activity becomes restricted to the medial part of the myotome where differentiation is underway (A'-C,F'-H). By E11.5, the expression of the reporter starts to turn off within this tissue at rostral levels of the axis (D,E,H'). Similarly, the expression of *Gli1* and *Ptch1* is strong within the myotome from E9.5 onwards (I'-K,M'-O) and starts to be downregulated at rostral levels of the axis from E11.5 (K',L,O',P). The levels of *Ptch1* expression are higher within the medial myotome than within its lateral domain (I'-K). The levels of *Gli1* expression were rather equally distributed throughout the myotome (O). Shh signaling in the dermyotome of mouse embryos is barely detectable. In this tissue, the GBS-GFP reporter activity is not detected (A-C,F-H) and very weak levels of *Gli1* and *Ptch1* can be observed at the brachial level of E9.5 (I',M') and E10.5 embryos (J,N). The sclerotome displays a ventral-to-dorsal gradient of Shh signaling that declines over time. At E9.5, all the markers for Shh signaling exhibit high levels of expression within the sclerotome part abutting the notochord, which progressively decreases along the medial lateral axis (F,F',I,I',M,M'). From E10.5, this gradient is no longer visible, GBS-GFP activity is downregulated (B,G) and *Gli1* and *Ptch1* mRNAs display weak levels of expression throughout the tissue (J,N). The black dashed lines delineate the myotome, the white dashed line separates the medial and lateral part of this tissue. Bracket marks the ventral domain of marker expression in sclerotome. Asterisks mark the dorsal root ganglia. In all panels, lateral is to the left and dorsal to the top. DM, dermomyotome; M, myotome; Scl, sclerotome. Scale bars: 50 µm.
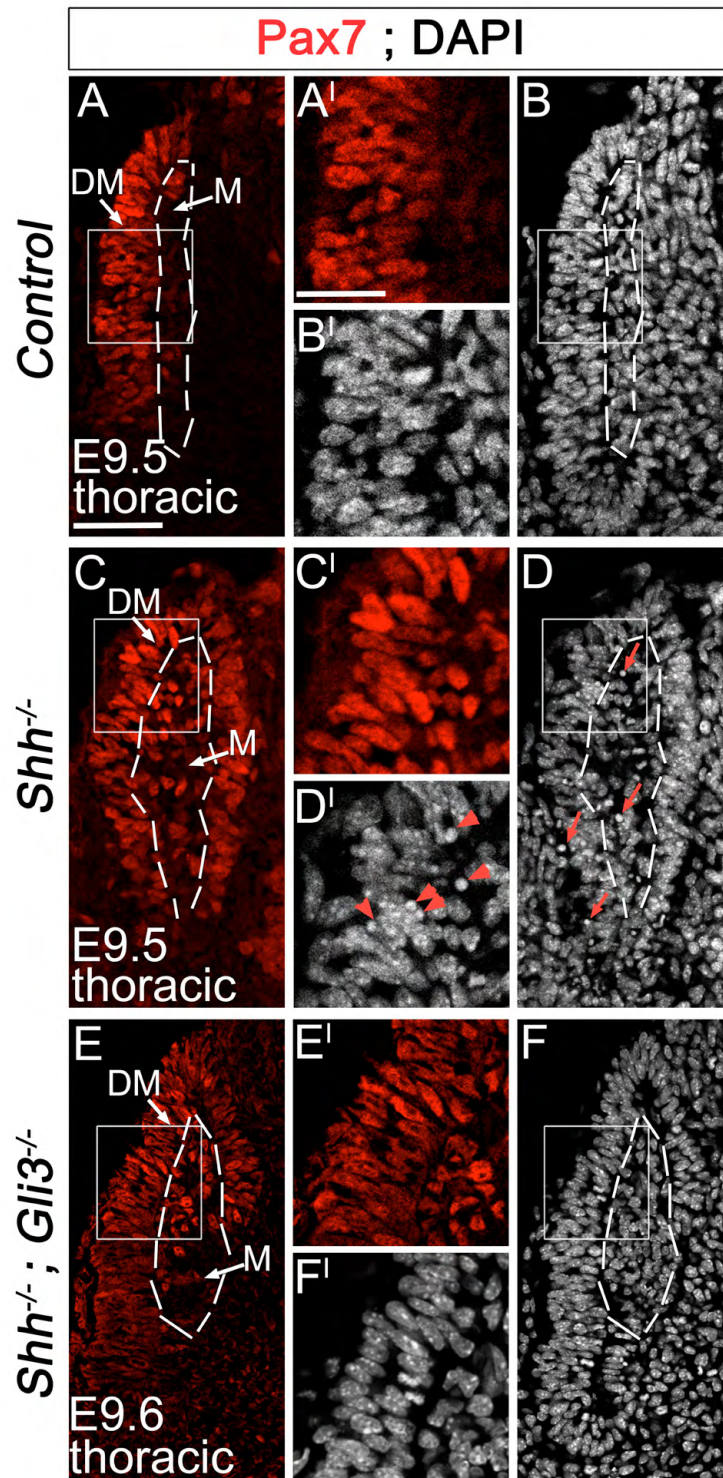
**Fig. S2. Enhanced Gli3 repressor activity contributes to the death of DM progenitors in *Shh* mutants.** (**A-F'**) Staining for Pax7 (red) and DAPI (gray) on transverse sections of E9.5 control (A-B'), *Shh*^{−/−} (C-D') and *Shh*^{−/−}; *Gli3*^{−/−} (E-F') mouse embryos at thoracic levels. The DM of *Shh* single mutants is unhealthy and displays numerous pyknotic figures (D,D'), which are absent from the DM of control embryos (B,B'). The loss of Gli3 function rescues the increase in cell-death observed in absence of *Shh* (F,F'). This supports the idea that Shh acts as a pro-survival factor on the DM by preventing high levels of Gli3 repressor activity. In absence of Shh ligand, most of myotome cells remain Pax7^{+}, whereas they tend in control embryos to differentiate and hence switch off Pax7. The myotome cells in E9.5 *Shh; Gli3* double mutants remain also Pax7^{+} as in *Shh* mutants, suggesting that the timing of differentiation is set not only by the removal of Gli3 repressor activity by Shh, but also by a positive activity of Gli transcription factors. This is consistent with the myotome cells presenting the highest levels of Shh signaling (see supplementary material Fig. S1). A', B', C', D', E' and F' are higher magnifications of the boxed areas in A, B, C, D, E and F, respectively. Arrows and arrowheads in D,D' point at pyknotic nuclei. The white dashed lines delineate the myotome. In all panels, lateral is to the left and dorsal to the top. DM, dermomyotome; M, myotome. Scale bars: in A, 50 µm for A-F; in A', 25 µm for A'-F'.
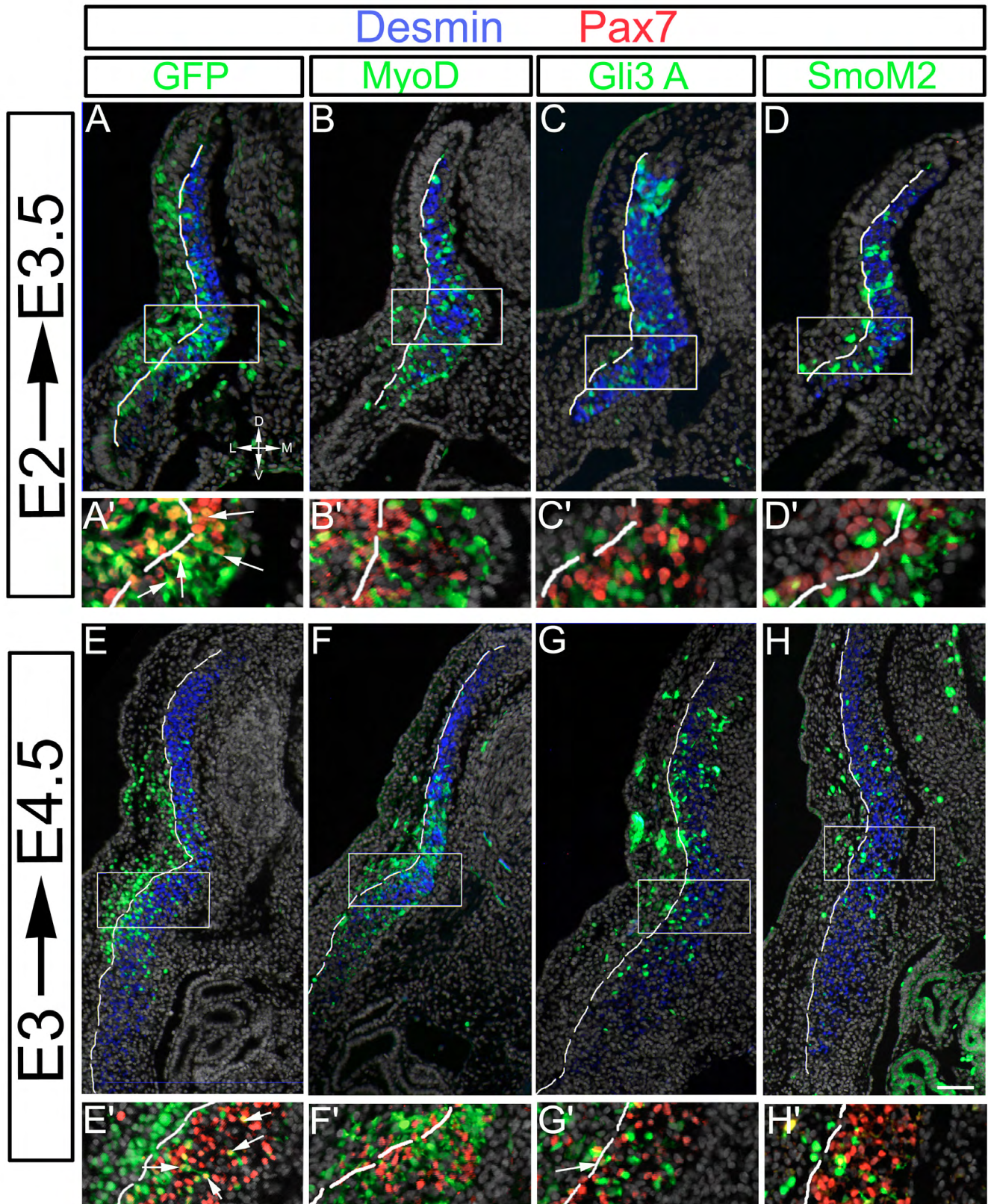
**Fig. S3. Downstream Shh signaling components stimulate myogenesis of DM progenitors that are refractory to Shh.** (**A-D'**) Transverse sections following electroporation of control GFP (A), MyoD (B), GliA (C) or SmoM2 (D) to the dorsal somite at E2. Desmin expression delineates the myotomes and the dashed line marks the boundary between the myotome and dermis. At E3.5, all genes enhanced myogenic differentiation at the expense of Pax7+ progenitors as most GFP+ cells are Pax7– compared with control in which many GFP+/Pax7+ cells are apparent (see A'-D', which represent enlargements of the boxed areas in A-D, respectively). Arrows in A' indicate cells co-expressing GFP and Pax7. (**E-H**) Equivalent treatments at E3 had a similar effect as at the young stage with few GFP+ progenitors co-expressing Pax7 compared with control GFP (see Fig. 7Q for quantification). Scale bar: in A-D, 50 μm; in E-H, 100 μm.